1 Supplementary material

The responses of the multivariate classifiers used for the $\Xi_{cc}^{++} \to \Lambda_c^+ K^- \pi^+ \pi^+$ and $\Xi_{cc}^{++} \to \Xi_c^+ \pi^+$ decays are shown in Fig. 3. The classifier for the $\Xi_{cc}^{++} \to \Lambda_c^+ K^- \pi^+ \pi^+$ decay is based on a Boosted Decision Tree (BDT) algorithm and the classifier for the $\Xi_{cc}^{++} \to \Xi_c^+ \pi^+$ decay is based on a Multilayer Perceptron (MLP).

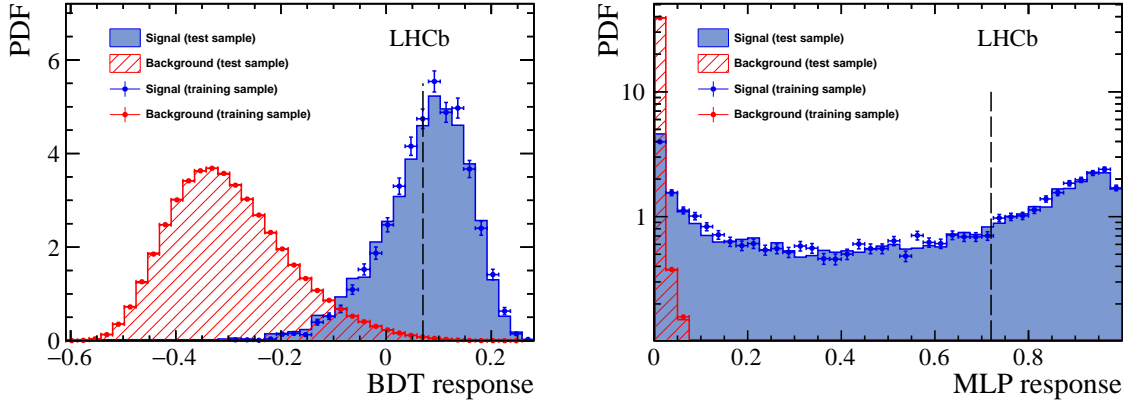Figure 3: Classifier outputs for (left) the $\Xi_{cc}^{++} \to \Lambda_c^+ K^- \pi^+ \pi^+$ decay, and (right) the $\Xi_{cc}^{++} \to \Xi_c^+ \pi^+$ decay. The black dashed lines indicate the optimised thresholds of selections.
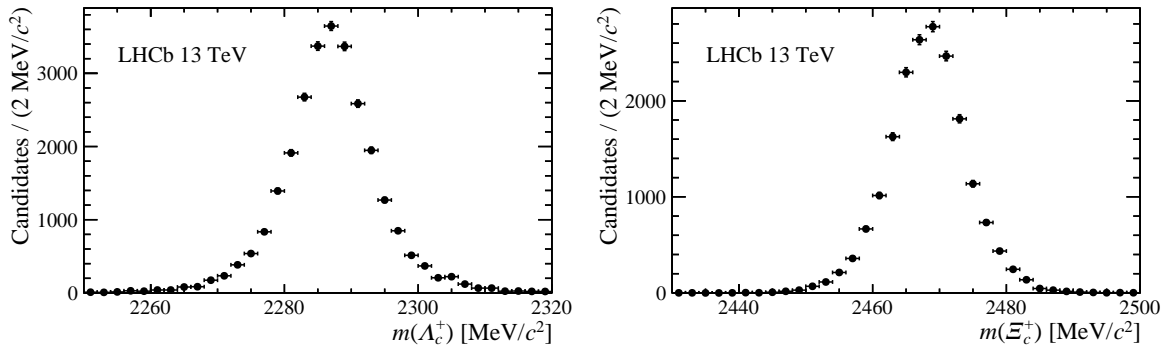

Figure 4: Mass distributions of (left) Λ_c^+ and (right) Ξ_c^+ candidates. The Λ_c^+ candidates are displayed for Ξ_{cc}^{++} candidates in a mass range from $3440 \, \mathrm{MeV}/c^2$ to $3770 \, \mathrm{MeV}/c^2$ and satisfying the BDT selection. The Ξ_c^+ candidates are in the Ξ_{cc}^{++} mass range from $3350 \, \mathrm{MeV}/c^2$ to $3800 \, \mathrm{MeV}/c^2$ and satisfy the MLP selection.

The mass distributions of Λ_c^+ and Ξ_c^+ candidates after the full selection are shown in Fig. 4. The $m_{\mathrm{cand}}(\Xi_{cc}^{++})$ mass distribution of the selected $\Xi_{cc}^{++} \to \Lambda_c^+ K^- \pi^+ \pi^+$ candidates in an enlarged mass range from $3440 \, \mathrm{MeV}/c^2$ to $3800 \, \mathrm{MeV}/c^2$ are shown in Fig. 5. The $m_{\mathrm{cand}}(\Xi_{cc}^{++})$ mass distribution of the selected $\Xi_{cc}^{++} \to \Lambda_c^+ K^- \pi^+ \pi^+$ candidates is shown in Fig. 6 in a wide mass range from $3400 \, \mathrm{MeV}/c^2$ to $5000 \, \mathrm{MeV}/c^2$ for 2016 and 2018 data. The 2017 data is not included as a mass cut of 3420–$3820 \, \mathrm{MeV}/c^2$ was introduced in the trigger for that year.
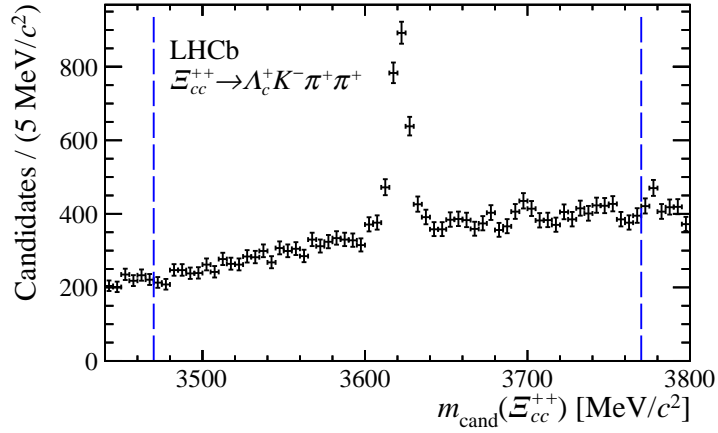
Figure 5: Mass distribution of the selected $\Xi_{cc}^{++} \to \Lambda_c^+ K^- \pi^+ \pi^+$ candidates in the mass range from $3440 \, \mathrm{MeV}/c^2$ to $3800 \, \mathrm{MeV}/c^2$. The blue dashed lines indicate the mass-fit window from $3470 \, \mathrm{MeV}/c^2$ to $3770 \, \mathrm{MeV}/c^2$.
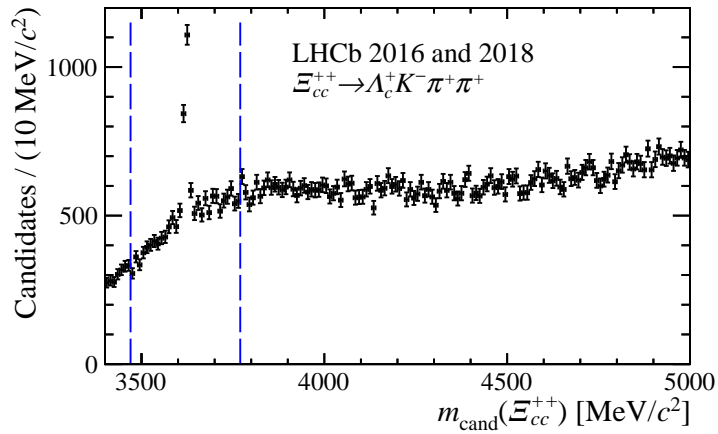

Figure 6: Mass distribution of the selected $\Xi_{cc}^{++} \to \Lambda_c^+ K^- \pi^+ \pi^+$ candidates in the mass range from $3800 \, \mathrm{MeV}/c^2$ to $5000 \, \mathrm{MeV}/c^2$. The blue dashed lines indicate the mass-fit window from $3470 \, \mathrm{MeV}/c^2$ to $3770 \, \mathrm{MeV}/c^2$.

2